Communications Biology

https://doi.org/10.1038/s42003-026-09920-4

Article in Press

A luminescent calcium biosensor enabling endpoint measurement of GPCR-mediated calcium signaling

Received: 27 October 2025

Accepted: 13 March 2026

Cite this article as: Doi, K., Kise, R., Shimizume, K. *et al.* A luminescent calcium biosensor enabling endpoint measurement of GPCR-mediated calcium signaling. *Commun Biol* (2026). https://doi.org/10.1038/s42003-026-09920-4

Kosuke Doi, Ryoji Kise, Kota Shimizume, Masataka Yanagawa & Asuka Inoue

Title:

A luminescent calcium biosensor enabling endpoint measurement of GPCR-mediated calcium signaling

Authors:

Kosuke Doi[1,2], Ryoji Kise[2.3], Kota Shimizume[2,3], Masataka Yanagawa[2,3,4], Asuka Inoue[2,3*]

Affiliations:

[1] Research & Development Section, Diagnostics Division, YAMASA Corporation, Choshi, 288-0056, Japan

[2] Graduate School of Pharmaceutical Sciences, Tohoku University, Sendai, 980-8578, Japan

[3] Graduate School of Pharmaceutical Sciences, Kyoto University, Kyoto 606-8501 Japan

[4] Cellular Informatics Laboratory, RIKEN Cluster for Pioneering Research, Wako 351-0198, Japan.

* Corresponding author: Asuka Inoue, Email: aska@pharm.kyoto-u.ac.jp

Abstract

$G_{q/11}$-coupled GPCRs regulate critical physiological processes through calcium mobilization, making intracellular Ca^{2+} dynamics a key readout for drug discovery and biomarker detection. However, the transient nature of calcium signals necessitates real-time monitoring with specialized equipment, creating barriers for high-throughput screening and limiting accessibility. Here we present CalLuc-2.1, a luminescent calcium biosensor that converts brief Ca^{2+} spikes into persistent luminescence changes readable tens of minutes after stimulation. By eliminating the need for precisely-timed detection, CalLuc-2.1 enables endpoint measurement of GPCR activation using standard plate readers. We demonstrate robust performance (Z' >0.88) across multiple $G_{q/11}$-coupled GPCRs in both agonist and antagonist screening formats. Furthermore, CalLuc-2.1 successfully detects endogenous GPCR ligands directly in human serum, offering a simpler alternative to immunoassays and mass spectrometry for biomarker quantification. This approach makes calcium-based GPCR assays accessible to any laboratory with basic luminescence detection capabilities, potentially accelerating both drug discovery and clinical research applications.

Introduction

G-protein–coupled receptors (GPCRs) are a large family of seven-transmembrane-domain proteins that transduce diverse extracellular stimuli into intracellular signals. Approximately 30% of drugs approved by the Food and Drug Administration target GPCRs, highlighting their significance as key pharmacological targets[1,2]. GPCR signaling is mediated by four major subclasses of heterotrimeric G proteins: G_s, $G_{i/o}$, $G_{q/11}$, and $G_{12/13}$[3].

Among these G-protein subclasses, members of the $G_{q/11}$ subfamily transduce signals by mobilizing inositol 1,4,5-triphosphate (IP_3) and intracellular calcium ions (Ca^{2+}) as second messengers, thereby regulating various physiological processes, including cell differentiation, proliferation, signal transduction, and muscle contraction[4,5]. Upon stimulation, $G_{q/11}$ proteins activate phospholipase Cβ, which hydrolyzes phosphatidylinositol 4,5-bisphosphate into IP_3 and diacylglycerol. IP_3 subsequently binds to its receptors in the endoplasmic reticulum (ER), triggering the release of Ca^{2+} and elevating cytosolic Ca^{2+} levels from approximately 100 nM at resting conditions to approximately 1 mM. Owing to its rapid and dynamic changes, intracellular Ca^{2+} is commonly monitored as a readout for $G_{q/11}$-coupled GPCR activation[5–8].

However, approaches for monitoring intracellular Ca^{2+} dynamics are often challenging due to complexities with measurement. Although tools such as small-molecule fluorescent calcium indicators or genetically encoded calcium indicators (GECIs) enable the real-time detection of transient Ca^{2+} changes within seconds, capturing such transient signals is experimentally demanding, along with instrumentation capable of acquiring data immediately after ligand addition[9–14]. To overcome these limitations, intracellular Ca^{2+} sensors that generate sustained signal outputs are preferable because they allow reliable measurements without specialized detection systems. Additionally, these sensors offer significant utility by circumventing the complexities of transient signal interpretation and streamlining endpoint assay workflows for high-throughput screening (HTS). Thus, engineering Ca^{2+} sensors with characteristics distinct from those of existing sensors has significant potential to broaden their utility in diverse applications.

The development of a biosensor that monitors Ca^{2+} signaling is a valuable tool for detecting the activation of $G_{q/11}$-coupled GPCRs and provides a practical platform for the indirect quantification of ligand concentrations in biological fluids. Recently, GloSensor-based assays that measure intracellular cAMP concentrations have been successfully applied to detect bioactive ligands in biological fluids by co-expressing G_s-coupled GPCRs and GloSensor in cultured cells[15–17]. This approach offers a powerful alternative to the traditional quantification methods for target analytes in biological samples. Unlike conventional methods such as immunoassays and mass spectrometry, which require complex procedures such as sample pretreatment and washing to mitigate interference from biological fluids, biosensor-based assays reduce these complexities. However, the current limitation is that the application of GloSensor is

restricted to G_s-coupled GPCRs because of its cAMP detection mechanism. For the detection of $G_{q/11}$-coupled GPCR, CalBiT that leverages the NanoBiT system combined with the Ca^{2+}-binding domain (CaBD) of calmodulin (CaM) has been developed[18]. However, CalBiT is not an optimal biosensor for assays using biological fluids. The development of biosensors that can detect the activation of $G_{q/11}$-coupled GPCRs in biological fluids will expand the applicability of biosensor-based assays for biomarker measurements.

In this study, we developed a Ca^{2+} biosensor, CalLuc-2.1, that generates a sustained luminescence signal from an initial Ca^{2+} spike. These properties provide a comparably simple and robust way to detect Ca^{2+} mobilization and are particularly advantageous for high-throughput and endpoint assays in multi-well plate formats. Our results demonstrated that CalLuc-2.1 not only expands the toolbox for detecting Ca^{2+} mobilization and $G_{q/11}$ signaling but also shows promise for future applications in measuring bioactive substances in biological fluids.

Results

Construction of split luciferase-based Ca^{2+} biosensors

To construct Ca^{2+} biosensors suitable for measuring ligands in biological samples, we selected bioluminescence as the detection modality owing to its suitability as a homogeneous assay platform. The advantages of bioluminescence assays include low background luminescence, resulting in high signal-to-noise ratios and enabling highly sensitive detection. In contrast, autofluorescence from biological samples and intrinsic fluorescence from test compounds may interfere with fluorescence-based assays, thereby increasing the risk of false positive and false-negative results[19]. Among the various luciferases commonly used in biosensor construction, such as firefly, *Gaussia*, *Renilla*, and deep-sea shrimp luciferases, such as NanoLuc, we chose firefly luciferase because of its lower susceptibility to interference from contaminants. Firefly luciferase requires magnesium ions (Mg^{2+}) and adenosine triphosphate to oxidize D-luciferin and emit bioluminescence[20]. Marine-derived luciferases often suffer from non-specific background luminescence in the presence of other proteins, such as albumin or insulin, because these luciferases do not require cofactors other than oxygen[21]. Recently, the development of CalBiT, a Ca^{2+} biosensor based on NanoBiT, a modified deep-sea shrimp luciferase, and CaBD of CaM, has been reported[18]. CalBiT detects $G_{q/11}$-coupled GPCR activation by measuring intracellular Ca^{2+} mobilization. We designed a split firefly luciferase system based on CalBiT, with fragments corresponding to residues 1–416 (designated as FLuc-N) and 395–550 (FLuc-C). These fragments were then fused to the CaBDs derived from human CaM or *Opsanus tau* troponin C. Because the CaM–M13 complex assembles through calcium-dependent conformational rearrangements of CaM, the spatial positioning of the split luciferase fragments relative to the CaM–M13 pair is a key determinant of fragment reconstitution efficiency. Based on this consideration,

we re-engineered CalLuc by permuting FLuc-N, FLuc-C, M13, and CaM, including swapping the luciferase halves, changing the CaM/M13 order, and evaluating linker variants of different lengths and flexibilities. Eight biosensor variants were generated by combining these components [Figure 1a].

We transiently expressed the eight Ca^{2+} biosensor constructs individually in HEK293A cells along with angiotensin II type 1 receptor (AT_1). The cells were loaded with D-luciferin for 2 h before the initial luminescence reading. Upon stimulation with 1 μM angiotensin II (AngII) via an injector equipped with a luminescent plate reader, the bioluminescence was measured for 20 min. A persistent decrease in the luminescent signal for up to 20 min was observed for seven of the eight constructs, except CalLuc-3, which displayed a unique response, with the signal returning to baseline levels within 2 min. This prolonged decrease in the kinetic pattern contrasts with the rapid attenuation of luminescence within 100 s previously reported for the Ca^{2+} sensor CalBiT[18]. Unlike CaM, TnC binds not only Ca^{2+} but also Mg^{2+}, suggesting that CalLuc-3 may behave differently from other sensors under reduced intracellular Ca^{2+} conditions [Supplementary Figure 1][22]. The NanoBiT components employed in CalBiT reportedly exhibited a K_D of 190 μM, K_{on} of 500 $M^{-1}s^{-1}$, and K_{off} of 0.2 s^{-1} (ref 23). The split firefly luciferase fragments in CalLuc were hypothesized to reassociate into a complementary conformation at a relatively slow rate following dissociation.

We modified the assay into a simplified operational format by leveraging the characteristic sustained CalLuc signal. Cells were stimulated by manually adding ligands using a multichannel pipette, and luminescence kinetics were recorded over a 20-min period [Figure 1b]. The decreased luminescence signals persisted throughout this time window, and ligand concentration–response curves were reliably generated using normalized signals recorded 18–20 min after post-stimulation [Figure 1c]. At early time points, the luminescence signal showed noticeable fluctuations, whereas it became markedly more stable after approximately 15 min, indicating that measurements obtained in this later phase were highly reproducible [Supplementary Figure 2]. Notably, the signals observed in cells treated with ionomycin, a calcium ionophore, indicated that CalLuc monitored intracellular Ca^{2+} concentration changes. YM-254890, a $G\alpha_q$ inhibitor, completely abolished agonist-induced CalLuc responses, whereas ionomycin-evoked signals remained unaffected. BAPTA-AM, an intracellular Ca^{2+} chelator, attenuated both agonist- and ionomycin-induced responses, although residual signals remained [Supplementary Figure 3]. Taken together, these findings indicate that CalLuc reports Ca^{2+} elevations in a manner dependent on both $G_{q/11}$-mediated signaling and increases in intracellular Ca^{2+} concentration, thereby demonstrating its effectiveness in detecting the activation of $G_{q/11}$-coupled GPCRs. For further validation, we selected CalLuc-2.1 due to its significantly larger signal window.

CalLuc-2.1 is capable of detecting intracellular Ca^{2+} mobilization downstream of various $G_{q/11}$-coupled

GPCRs

To assess its applicability across different $G_{q/11}$-coupled GPCRs, we tested four other receptors, covering diverse GPCR phylogenetic trees: orexin receptors (OX_1 and OX_2), oxytocin receptor (OT), and histamine H1 receptors (H_1). Upon stimulation with the corresponding endogenous agonists, all receptors elicited a decrease in ligand-induced luminescence signals, although the magnitude of the response varied across receptors [Figure 2a]. The luminescence kinetic curves were largely comparable to those of AT_1 [Supplementary Figure 4]. H_1 exhibited the highest efficacy among the five receptors. OX_1, OX_2, and AT_1 showed moderate efficacies, whereas OT showed the lowest efficacy. In contrast, the signals obtained from the mock cells showed no response to ligand stimulation. These results indicate that CalLuc-2.1 can detect various types of $G_{q/11}$-coupled GPCR activity. Next, we compared the sensitivity of the CalLuc-2.1-based assay with that of a commercially available Ca^{2+} assay. We used the FLIPR Calcium 6 kit, which uses a fluorescent Ca^{2+} indicator. HEK293A cells expressing each of the five GPCRs were stimulated with their corresponding agonists, and intracellular Ca^{2+} levels were measured. The FLIPR assay showed rapid signal elevation upon stimulation, returning to baseline within approximately 30 s, which is consistent with previous studies [Supplementary Figure 5][24]. The pEC_{50} values obtained from FLIPR and CalLuc assays were comparable for AT_1, H_1, OX_1, and OX_2. In contrast, a slight divergence was noted for OT. This result indicated that CalLuc-2.1 provides a sensitivity similar to that of the FLIPR Calcium 6 kit [Tables 1, 2 and Supplementary Figure 6].

Leveraging the characteristic sustained signal of CalLuc-2.1, we next investigated the reversibility of this signal by monitoring GPCR antagonism. HEK293A cells co-expressing AT_1 and CalLuc-2.1 were stimulated with 1 nM AngII, followed by the addition of the AT_1 antagonists, 1-sarcosine-8-isoleucine-angiotensin II (SI-AngII) or olmesartan (OMS). This assay protocol enables the evaluation of signal reversibility by adding an antagonist after agonist-induced activation. The results suggested that the decreased bioluminescence signals induced by agonist stimulation gradually recovered over time following antagonist treatment, consistent with the inhibition of AngII-mediated signaling [Figure 2b]. Additionally, in another assay, cells co-expressing AT_1 and CalLuc-2.1 were pre-treated with an AT_1 antagonist and subsequently stimulated with 1 nM AngII, resulting in an antagonist-concentration-dependent increase in signal responses [Figure 2c]. This result indicates that CalLuc-2.1 can detect both increases and decreases in $G_{q/11}$ signaling induced by both agonists and antagonists. This homogeneous end-point-compatible assay platform offers a simple method for evaluating antagonist activity.

To further assess the applicability of CalLuc as a research tool beyond $G_{q/11}$-coupled GPCRs, we examined whether the assay is compatible with chimeric G proteins and a promiscuous G protein, as is commonly employed in conventional Ca^{2+} assays to detect non-$G_{q/11}$-coupled GPCRs[25]. To evaluate whether CalLuc-2.1 can report Ca^{2+} responses via chimeric G proteins, we assessed four representative

$G_{i/o}$-coupled receptors; dopamine D2 receptor (D_2), serotonin receptor 1A (5-HT_{1A}), mu opioid receptor (μ), and alpha-2A adrenergic receptor (α_{2A}). For each receptor, we co-expressed CalLuc-2.1 together with either a chimeric $G\alpha_{q/i3}$ protein or the promiscuous G protein, $G\alpha_{16}$ (also known as $G\alpha_{15}$). In HEK293A cells co-expressing $G\alpha_{16}$, stimulation of α_2A or 5-HT_1A elicited sustained decreases in luminescence, a kinetic profile comparable to that observed for $G_{q/11}$-coupled receptors. By contrast, D_2 and μshowed either no detectable response or only a transient decrease in luminescence. In cells co-expressing $G\alpha_{q/i3}$, D_2 exhibited a sustained decrease in luminescence, consistent with the kinetic profile typically observed for $G_{q/11}$-coupled receptors, whereas the other receptors showed transient decreases followed by a subsequent rise in luminescence [Supplementary Figure 7 and 8]. These data demonstrate that CalLuc-2.1 can detect activation of a broad range of $G_{i/o}$-coupled GPCRs when paired with an appropriate G-protein partner, although the kinetic properties depend on the specific receptor–ligand combination.

CalLuc-2.1 enables the detection of a bioactive substance in biological fluids

To validate the robustness and high-throughput screening compatibility of the CalLuc-based assay, we evaluated the Z' factor, a statistical parameter that reflects assay robustness and reproducibility[26]. We assessed CalLuc-2.1 in two formats: agonist mode and antagonist mode. For the agonist assay, HEK293A cells expressing AT_1 were treated with angiotensin II (Ang II) or vehicle (48 wells per condition). The Z′-factor obtained from the CalLuc assay was 0.939 ± 0.003 (mean ± standard error of the mean (SEM); values hereafter are presented in the same format), whereas the FLIPR Ca^{2+} assay yielded a lower value of 0.647 ± 0.025. For the antagonist assay, HEK293A cells expressing AT_1 were pretreated with 100 nM olmesartan or vehicle and subsequently stimulated with 1 nM Ang II. Consistent with the agonist mode, the CalLuc-2.1 assay again produced a higher Z′-factor (0.882 ± 0.016) compared with the FLIPR Ca^{2+} assay (0.635 ± 0.055) [Table 3, Figure 3a, Supplementary Figure 9, and 10]. Since Z' factors above 0.5 are generally considered acceptable for HTS, our results suggest that the CalLuc-based assay system is well-suited for HTS in both agonist and antagonist format.

Next, we examined whether the assay could detect endogenous GPCR ligands in human biological fluids. We focused on lysophosphatidic acid (LPA), which is present in serum at concentrations of approximately 0.1–10 μM and produced by the action of autotaxin through preparation of serum from blood samples[27]. LPA acts on six LPA receptors ($LPA_{1–6}$), of which LPA_{1-5} are known to couple with $G_{q/11}$ proteins[28]. Using synthetic 1-oleoyl LPA, we measured the responses of six LPA receptors using a CalLuc-based assay. HEK293A cells were co-transfected with CalLuc-2.1 and each of the LPA receptors and exposed to buffer-diluted LPA, resulting in LPA_3 being the strongest activator of CalLuc signal among the

six LPA receptors [Figure 3b]. Next, we investigated the detection of LPA in the serum using LPA_3. HEK293A cells were co-transfected with CalLuc-2.1 and LPA_3 and subsequently exposed to four different human serum samples. In receptor-expressing cells, a decrease in luminescence signal was observed upon serum treatment. Notably, the LPA_3-dependent signals were mostly attenuated when the serum samples were pre-treated with dextran-coated charcoal (DCC), which can deplete low-molecular-weight compounds, including LPA, supporting the fact that the assay detects LPA itself [Figure 3c][29,30]. In contrast, mock-transfected cells did not exhibit a decrease in luminescence, indicating that the observed signal reduction was dependent on the expression of the introduced LPA_3 [Figure 3d]. Previous studies have reported endogenous expression of LPA receptors in HEK293A cells, and their activity can be detected with other assay formats; however, the CalLuc assay did not detect activation of these endogenous receptors, likely reflecting differences in assay principles and readout modalities. Although CalLuc employs intracellular Ca^{2+} as its detection modality and might therefore be expected to exhibit high sensitivity, our results suggest that its sensitivity is not insufficient under our conditions to detect signaling from endogenously expressed receptors[31]. To further validate the involvement of the $G_{q/11}$ pathway, we pre-treated the cells with YM-254890, a selective $G\alpha_{q/11}$ protein inhibitor[32]. Under these conditions, the serum-induced decrease in luminescence was completely abolished, confirming that the response was mediated by the $G_{q/11}$ signaling pathway [Figure 3c and 3d]. Furthermore, we quantified serum LPA concentrations using this method. A standard curve was generated using synthetic 1-oleoyl LPA and then applied to serum samples to calculate concentrations [Supplementary Figure 11]. The estimated values ranged from 0.17 to 0.61 μM (mean ± standard error of the mean (SEM): 0.35 ± 0.11 μM), consistent with previously reported serum LPA levels [Supplementary Figure 12]. These findings suggest that CalLuc-2.1 can detect endogenous ligands present in human serum.

Discussion

In this study, we developed CalLuc-2.1, a luminescent biosensor that detects intracellular Ca^{2+} elevation following the activation of $G_{q/11}$-coupled GPCRs, with the key advantages of simplicity and ease of implementation. Ca^{2+} mobilization assays and inositol monophosphate accumulation (IP_1) assays are established methods for detecting $G_{q/11}$-coupled GPCR activation. Whereas Ca^{2+} mobilization produces a rapid, transient, flux-type response, the IP_1 assay enables endpoint measurements because intracellular IP_1 accumulates and reaches equilibrium state within tens of minutes. Owing to this convenience, IP_1 assays are widely used for assessing $G_{q/11}$-mediated signaling[33]. Although CalLuc-2.1 is also a biosensor that detects intracellular Ca^{2+} elevation, it provides a homogeneous assay platform to detect $G_{q/11}$-coupled GPCRs with high robustness using standard luminescence plate readers and multichannel pipettes without requiring specialized

equipment, such as injector-equipped plate readers. The CalLuc-based assay is cost-effective and requires only transfected cells, assay buffer, D-luciferin, and the ligand. In a 96-well plate format, the CalLuc-2.1 assay yielded Z'-factors of 0.939 in the agonist assay and 0.882 in the antagonist assay, demonstrating excellent plate-assay performance and meeting the quality criteria for HTS assays. In comparison, the CalLuc-based assay produced higher the Z' factors than the FLIPR Ca^{2+} assay in both formats, further supporting its suitability for high-throughput screening applications. Beyond screening performance, CalLuc-2.1 also offers flexibility in assay configuration and signaling coverage, which is advantageous for GPCR-targeted drug discovery. In the antagonist format, agonist-induced luminescence suppression was detectable regardless of whether the antagonist was added before or after agonist stimulation. Moreover, by combining CalLuc-2.1 with chimeric Gα proteins, the assay can be extended to $G_{i/o}$-coupled GPCRs, thereby broadening its utility beyond $G_{q/11}$ signal pathways. However, because the performance of chimeric Gα proteins depends on their compatibility with individual receptors, careful selection of the appropriate chimeric Gα protein is required for each receptor of interest.

CalLuc, which detects changes in intracellular Ca^{2+} levels downstream of $G_{q/11}$-coupled GPCRs, detects a sustained signal that distinguishes it from other techniques. Although intracellular Ca^{2+} levels typically return to baseline within a few seconds after stimulation, CalLuc exhibits a sustained signal for at least 20 min[34]. This suggests that the CaBD retains its Ca^{2+}-bound conformation even after cytosolic Ca^{2+} levels return to their basal state. The prolonged signal attenuation of CalLuc contrasts with that of other CaBD-based sensors, such as CalBiT, which exhibit transient signals in response to intracellular Ca^{2+} mobilization[18]. The lack of such sustained signal attenuation in CalBiT, which has a nearly identical structure to CalLuc except for the luciferase component, implies that split firefly luciferase is the critical determinant of this phenomenon. Furthermore, the addition of antagonists led to a gradual recovery of the luminescent signal, returning it to near-baseline levels approximately 30 min after treatment. This finding suggests that antagonist-mediated inhibition of $G_{q/11}$ signaling prompts CaBD to revert to its Ca^{2+}-free conformation, thereby restoring the active state of CalLuc. As CaM is known to interact with various proteins and undergo post-translational modifications such as phosphorylation, these phenomena may influence the conformational dynamics of CaM[35,36]. These findings suggest that the distinctive sustained signal of CalLuc is not solely due to the kinetics of Ca^{2+} mobilization, but is also influenced by the structural properties of its luciferase fragment and its potential interaction with downstream signaling pathways.

While the preferred property of luminescent assays is an increased luminescent response, CalLuc-2.1 exhibits a decrease in the luminescent signal upon stimulation. We initially hypothesized that ligand-induced Ca^{2+} mobilization, which triggers a conformational change in the CaBD of CaM, leads to the reconstitution of split-firefly luciferase and a subsequent increase in luminescence. Contrary to this expectation, ligand stimulation resulted in a decreased luminescent signal, indicating that the split-firefly

luciferase existed in a reconstituted active state under basal conditions. The affinity of NanoBiT is approximately 190 μM, whereas that of split firefly luciferase is 10 μM[23]. Considering the substantially higher affinity of the split firefly luciferase fragments relative to the NanoBiT components, it is plausible that these fragments exhibited a degree of pre-association, regardless of the intracellular Ca^{2+} concentration[23]. Furthermore, the decrease in the luminescent signal implies that Ca^{2+}-induced conformational changes in the CaBD reduced the complementation of the split firefly luciferase fragments, leading to a loss of enzymatic activity. The CalLuc-based assay leverages the characteristic sustained signal of CalLuc to enable the high-throughput and convenient detection of $G_{q/11}$-GPCR activation.

Cell-based assays provide a useful platform for the measurement of bioactive substances in biological fluids. A prime example is the GloSensor-based assay, which has been successfully used to quantify G_s-coupled GPCR ligands[15–17]. Its clinical utility has been demonstrated in an assay for Graves' disease, where cells co-expressing the thyroid-stimulating hormone receptor and GloSensor-22F enabled the measurement of the activity of pathogenic thyroid-stimulating autoantibodies in patient serum[15,16]. This Glosensor-based assay has been approved by the regulatory agency in Japan for the in vitro diagnosis of Graves' disease and is used for routine diagnosis. The CalLuc-based assay developed in this study builds upon similar fundamental principles, along with distinct advantages such as the ability to detect the activation of $G_{q/11}$-coupled GPCRs. The decreased luminescence signal characteristic of CalLuc may present a disadvantage for measuring ligands in biological fluids. Since the amounts of interfering substances and contaminants in biological fluids vary by individual, non-specific signals may vary from specimen to specimen, interfering with accurate measurements. Although the CalLuc-based assay is a convenient method for measuring ligands in biological samples, the possibility of non-specific signals should be carefully considered. Given that the Guide to Pharmacology database lists 78 GPCRs that are primarily coupled to $G_{q/11}$, the CalLuc system holds significant potential as a valuable tool for the development of *in vitro* diagnostics[37].

The CalLuc-based assay overcomes many of the drawbacks of existing methods. It provides a simple, homogeneous, endpoint measurement for $G_{q/11}$ signaling that only requires co-transfection of the sensor with the receptor of interest, thereby avoiding the direct modification of signaling component proteins. Various techniques have been developed to detect GPCR signaling, although each has inherent limitations[38]. Protein-protein interaction-based methods, including Förster resonance energy transfer (FRET), bioluminescence resonance energy transfer (BRET), and luciferase complementation assays, enable homogeneous endpoint measurements but often require modifications to GPCRs, G proteins, or effector proteins, which can potentially introduce artifacts due to unexpected obstacles in intracellular signal transduction[39–44]. Reporter gene assays or the transforming growth factor-α shedding assay do not require the modifications, and can detect various signal transduction, but have drawbacks such as prolonged

incubation and complicated experimental procedure[45–48]. Other common assays also present challenges for high-throughput applications. For instance, fluorescence-based GECI like GCaMP, along with other fluorescent Ca^{2+} indicators, and other fluorescent, bioluminescent, FRET, or BRET-based Ca^{2+} biosensors are primarily suited for real-time detection rather than endpoint assays[11,18,49–55]. While the optimal assay must be selected based on specific experimental objectives, the unique features of CalLuc make it a useful tool for investigating G_q-mediated signaling.

In conclusion, CalLuc-2.1 is a valuable tool for diverse applications, including the study of the $G_{q/11}$ signaling pathway, high-throughput drug discovery, and the development of in vitro diagnostics.

Materials and Methods

Reagents

Orexin A, angiotensin II, oxytocin, and 1-sarcosine-8-isoleucine-angiotensin II were purchased from Peptide Institute (Osaka, Japan). Histamine, D-luciferin potassium salt, and YM-245890 were purchased from Fujifilm Wako Pure Chemicals (Osaka, Japan). LPA (18:1) was purchased from Avanti Research, Inc. (USA). Olmesartan was obtained from Merck (Germany).

Plasmid construction

Human codon-optimized genes for OX_1, OX_2, H_1, and all the CalLuc variants were synthesized by Eurofins Genomics. Flexi open reading frame clones of AT_1 and OT were purchased from Promega. All CalLuc genes were cloned into the pCAGGS vector (a kind gift from Dr. Jun-ichi Miyazaki of Osaka University, Japan). Detailed sequences of all CalLuc variants were listed in Supplementary Figure 13. OX_1, OX_2, H_1, AT_1, and OT constructs were fused to a hemagglutinin signal sequence, followed by a FLAG-linker-HiBiT-linker sequence (MKTIIALSYIFCLVFADYKDDDDKGGSGGGGSGGSSSGGGVSGWRLFKKISGGSGGGGSG) and cloned into the pCAGGS vector. Plasmids encoding LPA_1-LPA_6, μ, D2, α2A, $5\text{-}HT_{1A}$, chimeric $G\alpha_{q/i3}$ protein and promiscuous $G\alpha_{16}$ protein were used as described in previous reports[56].

Cell culture

HEK293A cells (Thermo Fisher Scientific, USA) were maintained in Dulbecco's modified Eagle's medium (DMEM), high glucose, and GlutaMAX Supplement (Thermo Fisher Scientific, USA) supplemented with 10% fetal calf serum (Thermo Fisher Scientific, USA) (complete DMEM). The cells were maintained in a humidified incubator at 37°C with 5% CO_2.

Transfection

Plasmid transfection was performed using either polyethyleneimine (PEI MAX; Polyscience, USA) or Lipofectamine 3000 (Thermo Fisher Scientific).

For the CalLuc-based assay, PEI MAX was used as the transfection reagent. HEK293A cells were seeded in a six-well plate at a density of 4.0×10^5 cells per well with 2 mL of complete DMEM and cultured for 1 day. For transfection, a PEI solution was prepared by mixing 5 μL of 1 mg/mL PEI MAX with 95 μL of Opti-MEM (Thermo Fisher Scientific, USA). The plasmid mixture, containing 200 ng of GPCR-encoding plasmid, 1 μg of CalLuc-encoding plasmid, and 1 μg of empty pCAGGS vector, was diluted in 100 μL of Opti-MEM. For CalLuc assays employing either the chimeric $G\alpha_{q/i3}$ protein or the promiscuous $G\alpha_{16}$ protein, cells were transfected with a plasmid mixture consisting of 200 ng of GPCR-encoding plasmid, 1 μg of

CalLuc-2.1-encoding plasmid, 100 ng of plasmid encoding either $G\alpha_{q/i3}$ or Gα16, and 900 ng of empty pCAGGS vector. The negative control, referred to as the mock control, was prepared by replacing the GPCR plasmid with an empty pCAGGS plasmid. The PEI solution and the plasmid mixture were combined and incubated for 20 min at room temperature. The resulting PEI–plasmid DNA complex was then added to the cells, which were cultured for 1 day before the assay.

For the FLIPR calcium assay, Lipofectamine 3000 was used for transfection. Cells were harvested with 0.05% trypsin-ethylene diamine tetraacetic acid (EDTA), centrifuged at 190×*g* for 5 min, and then suspended in 12 mL of DMEM containing 10% fetal calf serum. The plasmid mixture was prepared by combining 1 μg of GPCR-encoding plasmid, 2 μL of P3000 reagent, and 60 μL of Opti-MEM. A Lipofectamine solution was prepared by mixing 2.5 μL of Lipofectamine 3000 with 60 μL of Opti-MEM. The plasmid mixture and Lipofectamine solution were combined and incubated for 15 min at room temperature. The resulting Lipofectamine-plasmid DNA complex was added to the cell suspension, and the cells were seeded into a 96-well clear-bottom black plate.

CalLuc-based assay

The CalLuc-based assay was performed using a previously reported GloSensor-based assay with minor modifications. Briefly, transfected cells were washed with phosphate-buffered saline (PBS), harvested in PBS containing 1 mM EDTA, and centrifuged at 190×*g* for 5 min. The cell pellets were suspended in 1.2 mL of assay buffer (Hanks' balanced salt solution containing 0.01% bovine serum albumin and 5 mM HEPES at pH 7.4). Cells were then seeded into white 96-well plates at 40 μL per well, followed by the addition of 10 μL of D-luciferin solution (10 mM D-luciferin potassium salt diluted in assay buffer), resulting in a final concentration of 2 mM D-Luciferin. The plates were then incubated for 2 h in the dark at room temperature.

Initial luminescent counts were measured for 10 s using an injector-equipped luminescent plate reader (Infinite 200 Pro, TECAN, Switzerland). Subsequently, the vehicle (assay buffer) or agonist (1 μM angiotensin II) was added via the injectors, and the luminescent kinetics were measured for 100 s, and the fold-over-basal value was obtained.

For experiments using a luminescent plate reader (GloMax Explorer, Promega Corporation, USA) and a multichannel pipette for agonist addition, the initial luminescent counts were measured for 5 min. Subsequently, the vehicle (assay buffer) or agonist at appropriate concentrations was added using a multichannel pipette, the luminescent kinetics were measured for 20 min, and the fold-over-basal value was obtained. The mean fold-over-basal values at 18–20 min after agonist addition were calculated and normalized to those of vehicle-treated controls. These normalized values were plotted against the logarithm of the compound concentration, and concentration–response curves were fitted using a four-parameter

logistic model.

CalLuc-based antagonist assay

Antagonist evaluation using CalLuc-2.1 was performed with minor modifications to the standard CalLuc-based assay. Briefly, cells were harvested, suspended in 0.9 mL of assay buffer, and then seeded into white 96-well plates at 30 μL per well. Precisely 10 μL of D-luciferin solution (10 mM d-luciferin potassium salt diluted in assay buffer) was added to each well. Plates were incubated for 2 h in the dark at room temperature, and the initial luminescent counts were measured using a GloMax Explorer.

For antagonist treatment prior to agonist stimulation, cells were treated with SI-AngII or OMS at concentrations ranging from 1 pM to 100 nM. Luminescent kinetics were measured for 20 min before 100 nM AngII was added, followed by repeated measurement for 30 min.

For antagonist treatment after agonist stimulation, the cells were first treated with 100 nM Ang II. Luminescent kinetics were measured for 20 min, after which SI-AngII or OMS at final concentrations ranging from 1 pM to 100 nM were added, followed by an additional 30-min measurement of kinetics.

Detection of LPA in human serum using CalLuc-based assay

Four human serum samples were purchased from TRINA Bioreactives (Switzerland). DCC treatment for LPA depletion was performed as previously described[17].

The CalLuc-based assay was modified slightly to detect LPA in human serum. Harvested cells were suspended in 0.9 mL of assay buffer and seeded in white 96-well plates at a volume of 30 μL per well. Exactly 10 μL of d-luciferin solution was added to each well, and the plates were incubated for 2 h in the dark at room temperature. Precisely 30 min before the addition of human serum, cells were treated with vehicle (assay buffer) or 1 μM YM-245890. The initial luminescent counts were measured for 5 min using a GloMax Explorer. Subsequently, the cells were treated with human serum diluted 80-fold in the assay buffer. Luminescent kinetics were measured for 20 min, and the fold-over-basal value was calculated from the mean of an 18−20 min time window after serum addition.

Calculation of the Z' factor

The Z factor was calculated using a standard CalLuc-based assay. Following a 2-h incubation with D-luciferin, cells seeded in odd-numbered columns were treated with vehicle (assay buffer), while cells in even-numbered columns were treated with an agonist (100 nM AngII). Luminescence kinetics were measured for 20 min, and the fold-over-basal value was calculated from the mean of an 18−20 min time window after agonist (or vehicle) addition. The Z' factor was calculated as previously described[25].

FLIPR calcium assay

The FLIPR Calcium 6 Assay kit (Molecular Devices, USA) was dissolved at 0.6 mg/mL in the assay buffer. The medium was aspirated from cells cultured in 96-well clear-bottom black plates, and 80 μL of the FLIPR Ca 6 solution was added to each well. The cells were incubated for 90 min at 37°C humidified CO_2 incubator, then moved and incubated for an additional 30 min at room temperature. The fluorescence kinetics were measured using a pipette-equipped plate reader (FLEX Station 3; Molecular Devices). Initial fluorescence intensity was measured for 15 s (1.5 s/time point). Subsequently, 20 μL of vehicle or agonist at appropriate concentrations was added, and fluorescence kinetics were measured for an additional 105 s (1.5 s/time point). Fluorescence intensity was normalized to the mean fluorescence intensity before stimulation. Normalized peak response values following agonist addition were then further normalized to those of vehicle-treated controls. These normalized values were plotted against the logarithm of the compound concentration, and concentration–response curves were fitted using a four-parameter logistic model.

Statistics and reproducibility

The concentration–response curves were fitted to a four-parameter variable slope nonlinear regression model using GraphPad Prism 9 (GraphPad, UK). Absolute Hill slope values less than 1.5 were set accordingly. The negative logarithms of the half-maximal effective concentration (pEC_{50}) and maximum effect (E_{max}) values were obtained. The number of replicates for each experiment is indicated in the corresponding figure legends. A multiple comparison test was conducted using one-way analysis of variance with Dunnett's post-hoc test.

Data availability

Source data underlying graphs can be obtained from Supplementary Data. All other data are available from the corresponding author (or other sources, as applicable) on reasonable request.

Acknowledgments

We thank the members of Inoue Laboratory for critically reading and editing the manuscript. A.I. was funded by KAKENHI JP21H04791, JP24K21281 and JP25H01016 from the Japan Society for the Promotion of Science (JSPS); JP22ama121038 and JP22zf0127007 from the Japan Agency for Medical Research and Development (AMED); JPMJFR215T and JPMJMS2023 from the Japan Science and Technology Agency (JST); The Uehara Memorial Foundation. M.Y. was funded by KAKENHI JP24K01982, JP24H01266 and JP25H0132 from the JSPS; JPMJPR20EF from the JST; The Lotte

Foundation. We would like to thank Editage (www.editage.jp) for English language editing.

Author contributions

Conceptualization, A.I.;
Methodology, K.D., R.K., M.Y., A.I.;
Investigation, K.D., K.S.;
Formal analysis, K.D.;
Validation, K.D., R.K., M.Y.;
Visualization, K.D.;
Writing-original draft, K.D.;
Writing-review & editing, K.D., R.K., M.Y., A.I.;
Funding acquisition, A.I.;
Supervision, R.K., M.Y., A.I.;

Competing interests

K.D. is an employee of YAMASA Corporation. A patent application covering the CalLuc sensors described in this manuscript has been filed by YAMASA Corporation and Tohoku University, with K.D, R.K., and A.I. named as inventors (application no. JP2025/178464, pending). K.S. and M.Y. declare no potential competing interests.

References

1. Hauser, A. S., Attwood, M. M., Rask-Andersen, M., Schiöth, H. B. & Gloriam, D. E. Trends in GPCR drug discovery: new agents, targets and indications. *Nat. Rev. Drug Discov.* **16**, 829–842 (2017). 10.1038/nrd.2017.178, PubMed: 29075003.
2. Hauser, A. S. et al. Pharmacogenomics of GPCR drug targets. *Cell* **172**, 41–54.e19 (2018). 10.1016/j.cell.2017.11.033, PubMed: 29249361.
3. Milligan, G. & Kostenis, E. Heterotrimeric G-proteins: a short history. *Br. J. Pharmacol.* **147**(Suppl 1), S46–S55 (2006). 10.1038/sj.bjp.0706405, PubMed: 16402120.
4. Wettschureck, N. & Offermanns, S. Mammalian G proteins and their cell type specific functions. *Physiol. Rev.* **85**, 1159–1204 (2005). 10.1152/physrev.00003.2005, PubMed: 16183910.
5. Clapham, D. E. Calcium signaling. *Cell* **131**, 1047–1058 (2007). 10.1016/j.cell.2007.11.028, PubMed: 18083096.
6. Berridge, M. J. Inositol trisphosphate and diacylglycerol: two interacting second messengers. *Annu. Rev. Biochem.* **56**, 159–193 (1987). 10.1146/annurev.bi.56.070187.001111, PubMed: 3304132.
7. Kadamur, G. & Ross, E. M. Mammalian phospholipase C. *Annu. Rev. Physiol.* **75**, 127–154 (2013). 10.1146/annurev-physiol-030212-183750, PubMed: 23140367.
8. Gresset, A., Sondek, J. & Harden, T. K. The phospholipase C isozymes and their regulation. *Subcell Biochem.* **58** 61–94 (2012). 10.1007/978-94-007-3012-0_3, PubMed: 22403074
9. Paredes, R. M., Etzler, J. C., Watts, L. T., Zheng, W. & Lechleiter, J. D. Chemical calcium indicators. *Methods* **46**, 143–151 (2008). 10.1016/j.ymeth.2008.09.025, PubMed: 18929663.
10. Nakai, J., Ohkura, M. & Imoto, K. A high signal-to-noise Ca($^{2+}$) probe composed of a single green fluorescent protein. *Nat. Biotechnol.* **19**, 137–141 (2001). 10.1038/84397, PubMed: 11175727.
11. Miyawaki, A. et al. Fluorescent indicators for Ca2+based on green fluorescent proteins and calmodulin. *Nature* **388**, 882–887 (1997). 10.1038/42264, PubMed: 9278050.
12. Dana, H. et al. High-performance calcium sensors for imaging activity in neuronal populations and microcompartments. *Nat. Methods* **16**, 649–657 (2019). 10.1038/s41592-019-0435-6, PubMed: 31209382.
13. Ohkura, M. et al. Genetically encoded green fluorescent Ca^{2+} indicators with improved detectability for neuronal Ca^{2+} signals. *PLOS One* **7**, e51286 (2012). 10.1371/journal.pone.0051286, PubMed: 23240011.
14. Zhang, Y. et al. Fast and sensitive GCaMP calcium indicators for imaging neural populations. *Nature* **615**, 884–891 (2023). 10.1038/s41586-023-05828-9, PubMed: 36922596.
15. Miao, L. Y. et al. A rapid homogenous bioassay for detection of thyroid-stimulating antibodies based on a luminescent cyclic AMP biosensor. *J. Immunol. Methods* **501**, 113199 (2022).

10.1016/j.jim.2021.113199, PubMed: 34871593.

16. Hoshina, M. et al. Development and basic performance verification of a rapid homogeneous bioassay for agonistic antibodies against the thyroid-stimulating hormone receptor. *J. Immunol. Methods* **528**, 113655 (2024). 10.1016/j.jim.2024.113655, PubMed: 38447802.
17. Doi, K., Kawakami, K., Ikuta, T. & Inoue, A. A cAMP-biosensor-based assay for measuring plasma arginine-vasopressin levels. *Sci. Rep.* **14**, 9453 (2024). 10.1038/s41598-024-60035-4, PubMed: 38658606.
18. Yang, J. & Johnson, C. H. Bioluminescent sensors for Ca++ flux imaging and the introduction of a new intensity-based Ca++ sensor. *Front. Bioeng. Biotechnol.* **9**, 773353 (2021). 10.3389/fbioe.2021.773353, PubMed: 34778237.
19. Troy, T., Jekic-McMullen, D., Sambucetti, L. & Rice, B. Quantitative comparison of the sensitivity of detection of fluorescent and bioluminescent reporters in animal models. *Mol. Imaging* **3**, 9–23 (2004). 10.1162/15353500200403196, PubMed: 15142408.
20. Syed, A. J. & Anderson, J. C. Applications of bioluminescence in biotechnology and beyond. *Chem. Soc. Rev.* **50**, 5668–5705 (2021). 10.1039/d0cs01492c, PubMed: 33735357.
21. Vassel, N. et al. Enzymatic activity of albumin shown by coelenterazine chemiluminescence. *Luminescence* **27**, 234–241 (2012). 10.1002/bio.2357, PubMed: 22362656.
22. Rayani, K. et al. Binding of calcium and magnesium to human cardiac troponin C. *J. Biol. Chem.* **296**, 100350 (2021). 10.1016/j.jbc.2021.100350, PubMed: 33548225.
23. Dixon, A. S. et al. NanoLuc complementation reporter optimized for accurate measurement of protein interactions in cells. *ACS Chem. Biol.* **11**, 400–408 (2016). 10.1021/acschembio.5b00753, PubMed: 26569370.
24. Vetter, I. Development and optimization of FLIPR high throughput calcium assays for ion channels and GPCRs. *Adv. Exp. Med. Biol.* **740**, 45–82 (2012). 10.1007/978-94-007-2888-2_3, PubMed: 22453938.
25. Coward, P., Chan, S. D. H., Wada, H. G., Humphries, G. M. & Conklin, B. R. Chimeric G Proteins Allow a High-Throughput Signaling Assay of Gi-Coupled Receptors. *Anal. Biochem* 270, 242–248 (1999). 10.1006/abio.1999.4061, PubMed: 1033484126. ‘Zhang, J. H., Chung, T. D. & Oldenburg, K. R. A simple statistical parameter for use in evaluation and validation of high throughput screening assays. *J. Biomol. Screen.* **4**, 67–73 (1999). 10.1177/108705719900400206, PubMed: 10838414
27. Kano, K. et al. Suppressing postcollection lysophosphatidic acid metabolism improves the precision of plasma LPA quantification. *J. Lipid Res.* **62**, 100029 (2021). 10.1016/j.jlr.2021.100029, PubMed: 33524376.

28. Yung, Y. C., Stoddard, N. C. & Chun, J. LPA receptor signaling: pharmacology, physiology, and pathophysiology. *J. Lipid Res.* **55**, 1192–1214 (2014). 10.1194/jlr.R046458, PubMed: 24643338.
29. Ochi, Y., Shiomi, K., Hachiya, T., Yoshimura, M. & Miyazaki, T. Dextran-coated charcoal technique to make the hormone-free serum as a diluent for standard curve of radioimmunoassay. *Endocrinol. Jpn.* **20**, 1–7 (1973). 10.1507/endocrj1954.20.1, PubMed: 4353249.
30. Chen, R. F. Removal of fatty acids from serum albumin by charcoal treatment. *J. Biol. Chem.* **242**, 173–181 (1967). 10.1016/S0021-9258(19)81445-X, PubMed: 6016603.
31. Schihada, H., Shekhani, R. & Schulte, G. Quantitative assessment of constitutive G protein–coupled receptor activity with BRET-based G protein biosensors. *Sci. Signal.* (2021). 10.1126/scisignal.abf1653, PubMed: 34516756
32. Takasaki, J. et al. A novel Galphaq/11-selective inhibitor. *J. Biol. Chem.* **279**, 47438–47445 (2004). 10.1074/jbc.M408846200, PubMed: 15339913.33. Liu, K. et al. Comparison on Functional Assays for Gq-Coupled GPCRs by Measuring Inositol Monophospate-1 and Intracellular Calcium in 1536-Well Plate Format. Curr Chem Genomics 1, 70–78 (2008). 10.2174/1875397300801010070, PubMed: 20161830
34. Thomas, A. P., Bird, G. S., Hajnóczky, G., Robb-Gaspers, L. D. & Putney, J. W. Spatial and temporal aspects of cellular calcium signaling. *FASEB J.* **10**, 1505–1517 (1996). 10.1096/fasebj.10.13.8940296, PubMed: 8940296.
35. Yang, C.-F. & Tsai, W.-C. Calmodulin: the switch button of calcium signaling. *Tzu Chi Med. J.* **34**, 15–22 (2022). 10.4103/tcmj.tcmj_285_20, PubMed: 35233351.
36. Benaim, G. & Villalobo, A. Phosphorylation of calmodulin. Functional implications. *Eur. J. Biochem.* **269**, 3619–3631 (2002). 10.1046/j.1432-1033.2002.03038.x, PubMed: 12153558.
37. Harding, S. D. et al. The IUPHAR/BPS Guide to PHARMACOLOGY in 2024. *Nucleic Acids Res.* **52**, D1438–D1449 (2024). 10.1093/nar/gkad944, PubMed: 37897341.
38. Pearce, A. et al. Quantitative approaches for studying G protein-coupled receptor signalling and pharmacology. *J. Cell Sci.* **138**, JCS263434 (2025). 10.1242/jcs.263434, PubMed: 39810711.
39. Olsen, R. H. J. et al. TRUPATH, an open-source biosensor platform for interrogating the GPCR transducerome. *Nat. Chem. Biol.* **16**, 841–849 (2020). 10.1038/s41589-020-0535-8, PubMed: 32367019.
40. Littmann, T., Ozawa, T., Hoffmann, C., Buschauer, A. & Bernhardt, G. A split luciferase-based probe for quantitative proximal determination of Gαq signalling in live cells. *Sci. Rep.* **8**, 17179 (2018). 10.1038/s41598-018-35615-w, PubMed: 30464299.
41. Bünemann, M., Frank, M. & Lohse, M. J. Gi protein activation in intact cells involves subunit rearrangement rather than dissociation. *Proc. Natl Acad. Sci. U. S. A.* **100**, 16077–16082 (2003).

10.1073/pnas.2536719100, PubMed: 14673086.

42. Galés, C. et al. Real-time monitoring of receptor and G-protein interactions in living cells. *Nat. Methods* **2**, 177–184 (2005). 10.1038/nmeth743, PubMed: 15782186.
43. Malik, R. U. et al. Detection of G protein-selective G protein-coupled receptor (GPCR) conformations in live cells. *J. Biol. Chem.* **288**, 17167–17178 (2013). 10.1074/jbc.M113.464065, PubMed: 23629648.
44. Wright, S. C. et al. Conformation- and activation-based BRET sensors differentially report on GPCR-G protein coupling. *Sci. Signal.* **17**, eadi4747 (2024). 10.1126/scisignal.adi4747, PubMed: 38889226.
45. Cheng, Z. et al. Luciferase reporter assay system for deciphering GPCR pathways. *Curr. Chem. Genomics.* **4**, 84–91 (2010). 10.2174/1875397301004010084, PubMed: 21331312.
46. Lytton, S. D., Li, Y., Olivo, P. D., Kohn, L. D. & Kahaly, G. J. Novel chimeric thyroid-stimulating hormone-receptor bioassay for thyroid-stimulating immunoglobulins. *Clin. Exp. Immunol.* **162**, 438–446 (2010). 10.1111/j.1365-2249.2010.04266.x, PubMed: 21070207.
47. Wang, L. Y. et al. Development of a robust reporter gene-based assay for the bioactivity determination of recombinant human follicle stimulating hormone (rhFSH) pharmaceutical products. *J. Pharm. Biomed. Anal.* **177**, 112855 (2020). 10.1016/j.jpba.2019.112855, PubMed: 31561061.
48. Inoue, A. et al. TGFα shedding assay: an accurate and versatile method for detecting GPCR activation. *Nat. Methods* **9**, 1021–1029 (2012). 10.1038/nmeth.2172, PubMed: 22983457.
49. Thestrup, T. et al. Optimized ratiometric calcium sensors for functional in vivo imaging of neurons and T lymphocytes. *Nat. Methods* **11**, 175–182 (2014). 10.1038/nmeth.2773, PubMed: 24390440.
50. Saito, K. et al. Luminescent proteins for high-speed single-cell and whole-body imaging. *Nat. Commun.* **3**, 1262 (2012). 10.1038/ncomms2248, PubMed: 23232392.
51. Yang, J. et al. Coupling optogenetic stimulation with NanoLuc-based luminescence (BRET) Ca++ sensing. *Nat. Commun.* **7**, 13268 (2016). 10.1038/ncomms13268, PubMed: 27786307.
52. Qian, Y., Rancic, V., Wu, J., Ballanyi, K. & Campbell, R. E. A bioluminescent Ca^{2+} indicator based on a topological variant of GCaMP6s. *ChemBioChem* **20**, 516–520 (2019). 10.1002/cbic.201800255, PubMed: 29934970.
53. Farhana, I., Hossain, M. N., Suzuki, K., Matsuda, T. & Nagai, T. Genetically encoded fluorescence/bioluminescence bimodal indicators for Ca^{2+} imaging. *ACS Sens.* **4**, 1825–1834 (2019). 10.1021/acssensors.9b00531, PubMed: 31276380.
54. Oh, Y. et al. An orange calcium-modulated bioluminescent indicator for non-invasive activity imaging. *Nat. Chem. Biol.* **15**, 433–436 (2019). 10.1038/s41589-019-0256-z, PubMed: 30936501.
55. Suzuki, K. et al. Five colour variants of bright luminescent protein for real-time multicolour bioimaging. *Nat. Commun.* **7**, 13718 (2016). 10.1038/ncomms13718, PubMed: 27966527.
56. Inoue, A. et al. Illuminating G-Protein-Coupling Selectivity of GPCRs. Cell 177, 1933-1947.e25

(2019). 10.1016/j.cell.2019.04.044, PMID: 31160049

Figure 1

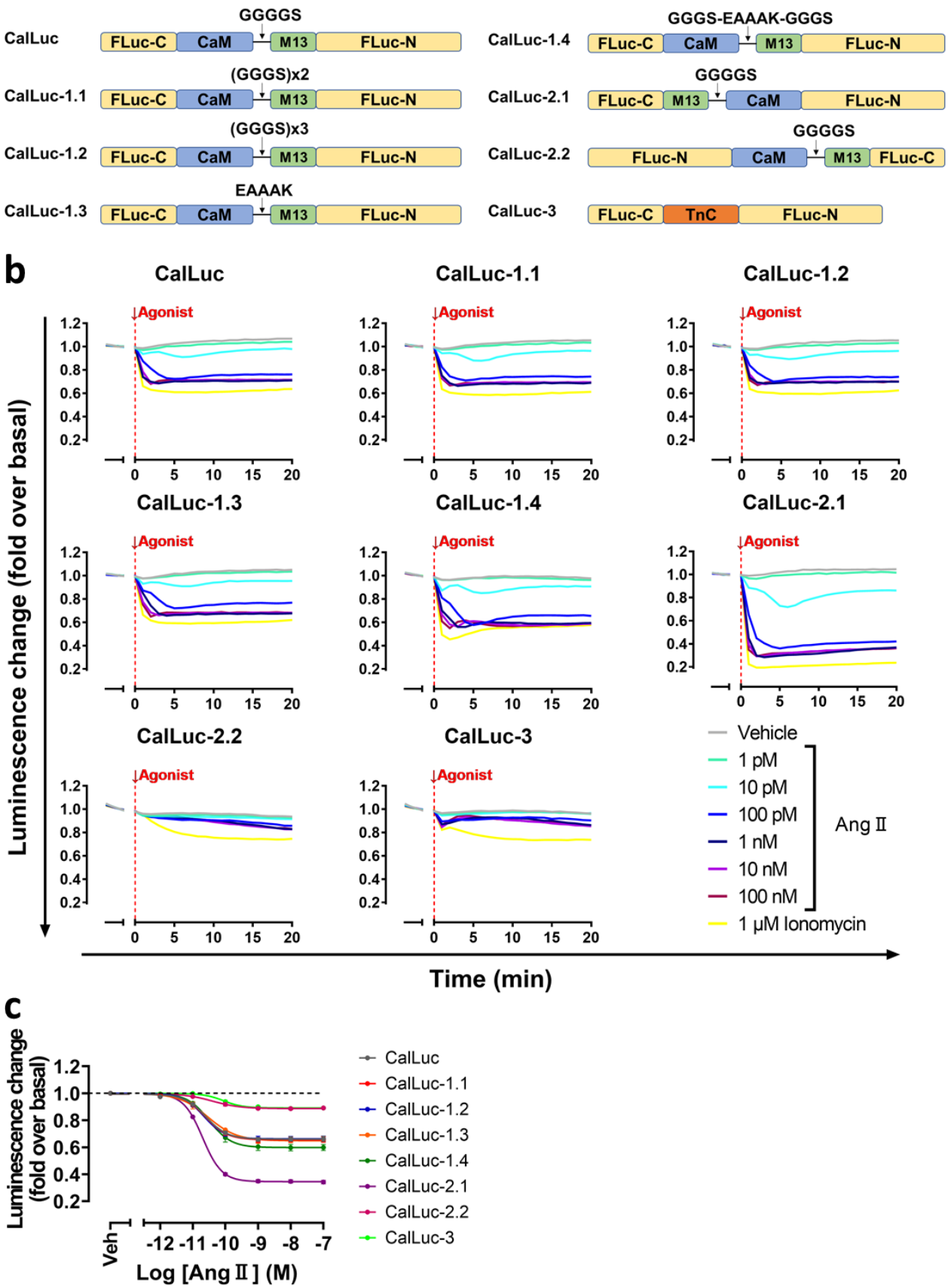
a
CalLuc
GGGGS
FLuc-C
CaM
M13
FLuc-N
CalLuc-1.1
(GGGS)x2
CalLuc-1.2
(GGGS)x3
CalLuc-1.3
EAAAK
CalLuc-1.4
GGGS-EAAAK-GGGS
CalLuc-2.1
CalLuc-2.2
CalLuc-3
TnC
b
CalLuc
CalLuc-1.1
CalLuc-1.2
CalLuc-1.3
CalLuc-1.4
CalLuc-2.1
CalLuc-2.2
CalLuc-3
Agonist
Luminescence change (fold over basal)
Time (min)
Vehicle
1 pM
10 pM
100 pM
1 nM
10 nM
100 nM
Ang Ⅱ
1 μM Ionomycin
c
Luminescence change (fold over basal)
Veh
-12 -11 -10 -9 -8 -7
Log [Ang Ⅱ] (M)
CalLuc
CalLuc-1.1
CalLuc-1.2
CalLuc-1.3
CalLuc-1.4
CalLuc-2.1
CalLuc-2.2
CalLuc-3

Figure 1. Construction of split luciferase-based Ca^{2+} biosensors.

(**a**) Schematic illustrations of the tested CalLuc biosensors.

(**b**) Luminescence kinetics of cells co-expressing AT_1 and each biosensor, measured using a luminescent plate reader and a multichannel pipette. Cells were stimulated with serially diluted AngII concentrations. Luminescence curves represent the mean of triplicates as biological replicates for each ligand.

(**c**) Concentration–response curves of the cells co-expressing AT_1 and each biosensor. Symbols and error bars represent the mean and standard error of the mean, respectively, of three independent experiments with each performed in duplicate. AT_1, angiotensin II type 1 receptor; CalLuc-2.1, Ca^{2+} biosensor; SEM, standard error of the mean; Veh, vehicle.

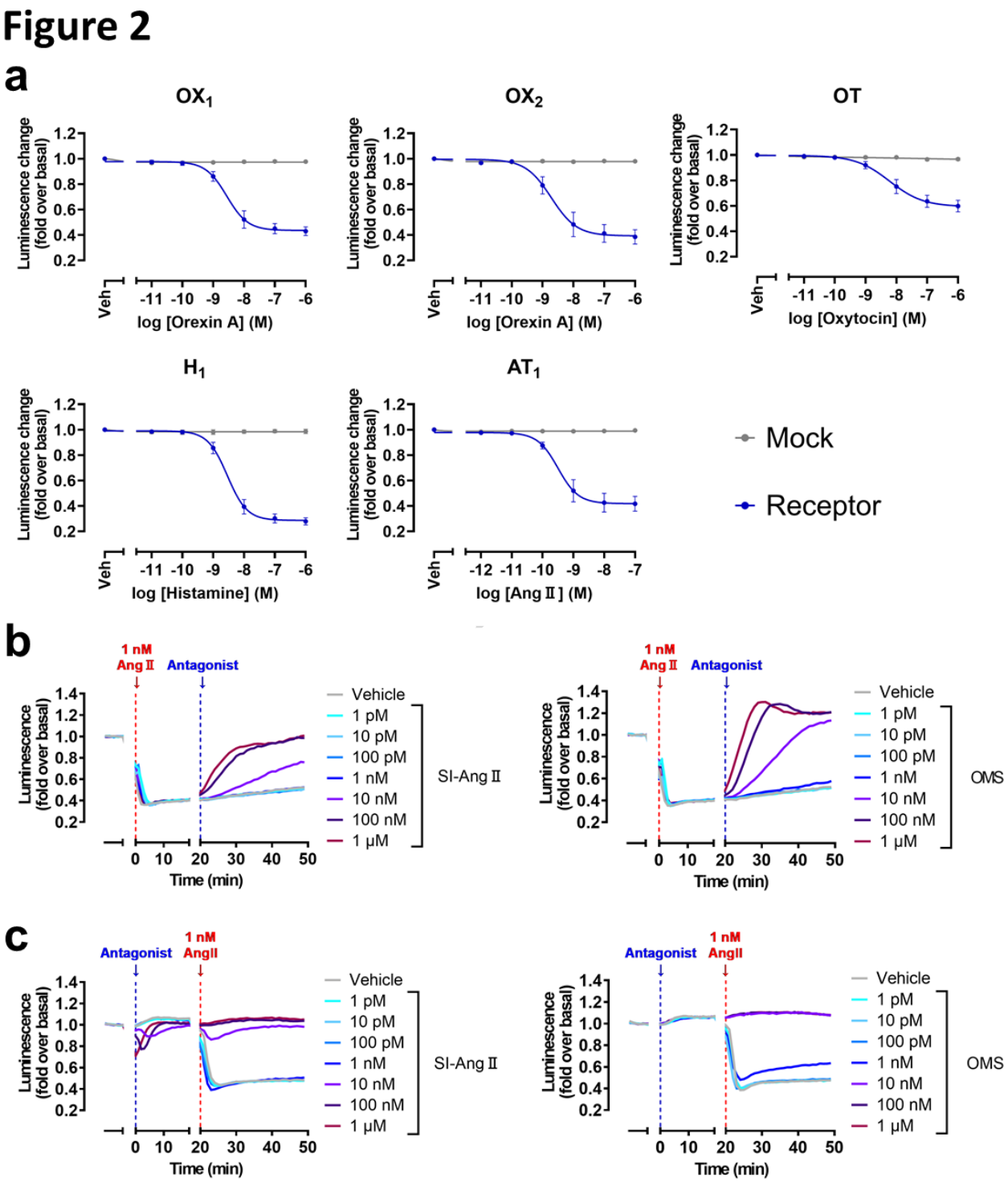

Figure 2. Detection of intracellular Ca^{2+} mobilization downstream of various $G_{q/11}$-coupled GPCRs by CalLuc-2.1.

(**a**) Concentration–response curves of tested $G_{q/11}$-coupled GPCRs in the CalLuc-based assay. Symbols and

error bars represent the mean and SEM from three independent experiments, each performed in duplicate.

(**b**) Representative luminescence kinetics of cells co-expressing AT_1 and CalLuc-2.1. Cells were pre-treated with agonists 20 min before antagonist addition. Curves represent the mean of duplicates as technical replicates for each antagonist.

(**c**) Representative luminescence kinetics of cells co-expressing AT_1 and CalLuc-2.1. Cells were pre-treated with antagonists 20 min before agonist addition. Curves represent the mean of duplicates as technical replicates for each condition. AT_1, angiotensin II type 1 receptor; GPCR, G-protein-coupled receptor; LPA, lysophosphatidic acid; CalLuc-2.1, Ca^{2+} biosensor; SEM, standard error of the mean; Veh, vehicle.

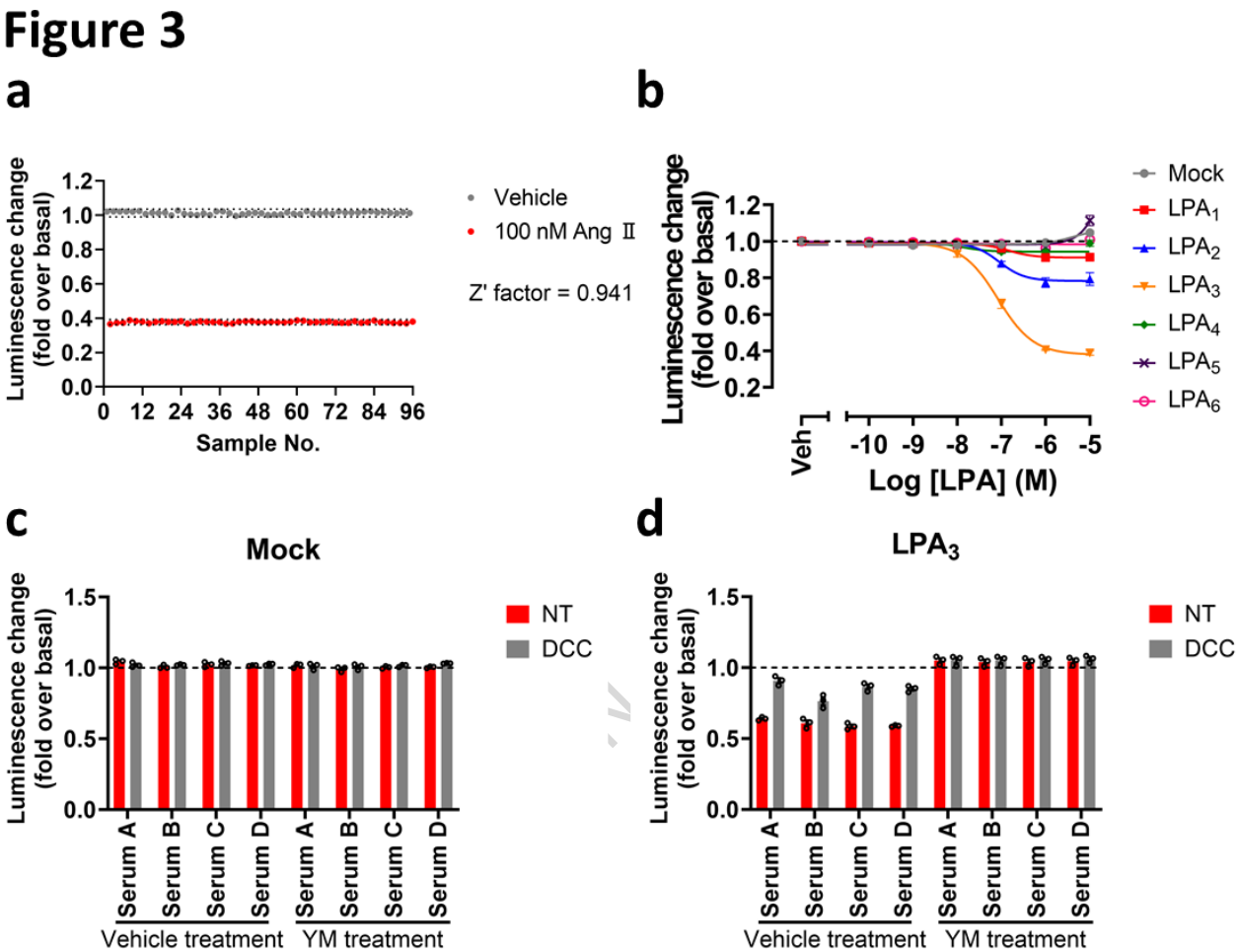

Figure 3. Detection of a bioactive substance in biological fluids using CalLuc-2.1 assay.

(**a**) Calculation of Z'-factor using cells co-expressing AT_1 and CalLuc-2.1. Symbols represent relative luminescence units obtained from single wells in a 96-well plate. Dotted lines indicate the range of mean ± 3× standard deviation (SD). The experiment was performed in triplicate as technical replicates. Z'-factors from three independent experiments are shown in Table 3. A representative result from experiment #1 is shown in this panel; experiments #2 and #3 are shown in Supplementary Figure 9.

(**b**) Concentration–response curves of six LPA receptors. Cells co-expressing CalLuc-2.1 and each LPA receptor were stimulated with serially diluted LPA. Symbols and error bars represent the mean and SEM from three independent experiments, each performed in duplicate.

(**c, d**) Detection of LPA in human serum using the CalLuc-based assay with cells co-expressing CalLuc-2.1 and mock-transfected (**c**) or LPA_3-expressing cells (**d**). Symbols represent data from three independent experiment. Bars and error bars indicate the mean and SEM, respectively, from three independent experiments performed in duplicate. Signals from cells pre-treated with YM-245890 were comparable to those from mock

cells. AT_1, angiotensin II type 1 receptor; LPA, lysophosphatidic acid; CalLuc-2.1, Ca^{2+} biosensor; YM, YM-254890; SEM, standard error of the mean.

Table 1. pEC_{50} values comparison among five receptors using the CalLuc-2.1 and the FLIPR-based assays.

pEC_{50}	AT_1	H_1	OX_1	OX_2	OT
FLIPR	9.43 ± 0.06	8.95 ± 0.30	8.46 ± 0.19	8.69 ± 0.08	9.04 ± 0.27
CalLuc	9.48 ± 0.12	8.54 ± 0.12	8.54 ± 0.17	8.66 ± 0.21	8.20 ± 0.19

Data are mean ± SEM from three independent experiments. pEC_{50}, negative logarithm of EC_{50} (half maximal effective concentration); CalLuc, Ca^{2+} biosensor; AT_1, angiotensin II type 1 receptor; OX_1, orexin receptor type 1; OX_2, orexin receptor type 2; OT, oxytocin receptor; H_1, histamine H1 receptor.

Table 2. E_{max} values comparison among five receptors using the CalLuc-2.1 and the FLIPR-based assays.

E_{max}	AT_1	H_1	OX_1	OX_2	OT
FLIPR	0.80 ± 0.14	0.66 ± 0.15	0.52 ± 0.09	0.45 ± 0.20	0.68 ± 0.10
CalLuc	0.57 ± 0.06	0.71 ± 0.04	0.54 ± 0.05	0.60 ± 0.06	0.40 ± 0.05

Data are mean ± SEM from three independent experiments. E_{max}, maximal effect relative to the baseline signals; CalLuc, Ca^{2+} biosensor; AT_1, angiotensin II type 1 receptor; OX_1, orexin receptor type 1; OX_2, orexin receptor type 2; OT, oxytocin receptor; H_1, histamine H1 receptor.

Table 3. Z'-factors for the CalLuc-based and the FLIPR-based assay.

		Exp. #1	Exp. #2	Exp. #3	Mean ± SEM
Agonist	CalLuc	0.941	0.942	0.933	0.939 ± 0.003
	FLIPR	0.696	0.636	0.610	0.647 ± 0.025
Antagonist	CalLuc	0.882	0.855	0.910	0.882 ± 0.016
	FLIPR	0.576	0.584	0.746	0.635 ± 0.055

SEM, standard error of the mean; Exp, experiment.

Editor's Summary

A luminescent calcium biosensor, CalLuc-2.1 converts transient Ca^{2+} spikes into stable signals, enabling simple endpoint assays for Gq/11-coupled GPCR drug screening and direct detection of endogenous ligands in human serum.

Peer Review Information
Communications Biology thanks the anonymous reviewers for their contribution to the peer review of this work. Primary Handling Editors: Dr Yi Chen and Dr Ophelia Bu. A peer review file is available.